Quadrupole Coupling and Knight Shift Anisotropy in "hcp" Lanthanum*

D. R. TORGESON AND R. G. BARNES
Institute for Atomic Research and Department of Physics, Iowa State University, Ames, Iowa
(Received 20 May 1964)

The nuclear magnetic resonance of La^{139} has been observed in hcp polycrystalline lanthanum metal at 25.6 kOe and 300°K. The recorded pattern at 15.5 Mc/sec displays a central line and one pair of satellite lines. The position and shape of the central line yields an isotropic Knight shift of $(0.685\pm0.020)\%$ and an axial shift of $(0.046\pm0.020)\%$. The satellite spacing yields a lowest pure quadrupole frequency $\nu_Q=101\pm4$ kc/sec or $e^2qQ/h=(1.41\pm0.06)$ Mc/sec. A calculation of the lattice electric field gradient is made for the $ABAC$ stacking sequences, yielding 0.540×10^{22} and 0.487×10^{22} cm^{-3} for the so-called A and B (or C) layer sites, respectively, by the method of plane-wise summation of de Wette. Improved values of the nuclear electric quadrupole moment, $Q(La^{139})=0.21$ b, and the Sternheimer antishielding factor, $\gamma_\infty(La^{3+})=-73.5$, are adopted and discussed. The sign of the conduction-electron electric field gradient is shown to be negative.

INTRODUCTION

NUCLEAR magnetic resonance (NMR) has been observed in the following hcp metals: beryllium,[1] magnesium,[2] scandium,[3–5] cobalt,[6] yttrium,[7,8] technetium,[9] cadmium,[10–12] lanthanum,[3,13] and thallium.[14] The hcp structure has axial symmetry along the c axis which permits an axially symmetric electric field gradient (EFG),[15] an axially symmetric anisotropic Knight shift,[16] or a combination of these two effects.[17] Yttrium, cadmium, and thallium have isotopes with spin $I=\frac{1}{2}$ only, and thus do not demonstrate quadrupole effects, although anisotropic shift effects are observed.[8,10–12,14] Beryllium has an exceedingly small Knight shift[1] and apparently an equally small axial Knight shift.[18] Cobalt is a special case in that it is a ferromagnetic metal and the NMR studies[6] have been done using zero (external) field. These experiments on cobalt did not yield Knight shift parameters or quadrupole splittings. The NMR of Sc^{45} in scandium and La^{139} in lanthanum metal was first reported by Blumberg *et al.*,[3] although these authors failed to detect any evidence of quadrupole interactions. Recently, quadrupole effects have been seen in scandium[4,5] and lanthanum.[13] In the present work we report the observation of the NMR of La^{139} in the double hcp lanthanum metal structure. The isotropic and axial Knight shifts and nuclear electric quadrupole interaction were measured in lanthanum. From a comparison of the observed and calculated electric field gradients, it is shown that a large conduction electron electric field gradient can exist in the double hcp structure of lanthanum, and furthermore, this electronic gradient is negative and opposes the lattice gradient.

EXPERIMENT

The lanthanum sample used in these studies consisted of about 3 g of 200-mesh lanthanum metal filings from a chunk of 99.9% pure lanthanum metal (produced in the Ames Laboratory). The filings were produced in a dry argon atmosphere in a stainless steel vacuum dry box. The data were obtained with a Varian V 4200 wide-line NMR spectrometer and a Harvey-Wells L-158 electromagnet equipped with hyperco pole tips. The magnetic field scan was calibrated with the La^{139} NMR in an $LaCl_3$ solution, and the Knight shift measurements were also made with respect to this reference solution. Frequencies were measured with a Computer Measurements Corporation 737 CN frequency counter.

The NMR recordings of the fresh filings showed a single asymmetric absorption derivative signal with a Knight shift of 0.63%. Heating of the sealed sample was begun at 140°C and thereafter at 10°C intervals until 220°C was reached. The resonance experiments were attempted after each anneal.

After the initial heating no resonance lines were observed. Not until after the 180°C anneal were any resonance lines identified. No apparent change in the observed pattern occurred after the 190, 200, 210, and

* Contribution No. 1510. Work was performed in the Ames Laboratory of the U. S. Atomic Energy Commission.
[1] W. D. Knight, Phys. Rev. **92**, 539 (1953).
[2] T. J. Rowland, in *Progress in Material Science*, edited by Bruce Chalmers (Pergamon Press, Inc., New York, 1961), Vol. 9.
[3] W. E. Blumberg, J. Eisinger, V. Jaccarino, and B. T. Matthias, Phys. Rev. Letters **5**, 52 (1960).
[4] S. L. Segel and R. G. Barnes, Bull. Am. Phys. Soc. **7**, 537 (1962).
[5] D. R. Torgeson, S. L. Segel, and R. G. Barnes (to be published).
[6] Louis E. Toth and S. Frederich Ravitz, Phys. Chem. Solids **24**, 1203 (1963).
[7] W. H. Jones, Jr., T. P. Graham, and R. G. Barnes, Acta Met. **8**, 663 (1960).
[8] R. G. Barnes, F. Borsa, S. L. Segel, and D. R. Torgeson (to be published).
[9] William H. Jones, Jr. and Frederich J. Milford, Phys. Rev. **125**, 1259 (1962).
[10] T. J. Rowland, Phys. Rev. **103**, 1670 (1956); Y. Masuda, J. Phys. Soc. Japan **12**, 523 (1957).
[11] Harlan E. Schone, Bull. Am. Phys. Soc. **8**, 592 (1963).
[12] F. Borsa and R. G. Barnes (to be published).
[13] D. R. Torgeson, D. Peterson, and R. G. Barnes, Bull. Am. Phys. Soc. **8**, 529 (1963).
[14] N. Bloembergen and T. J. Rowland, Phys. Rev. **97**, 1679 (1955).
[15] R. V. Pound, Phys. Rev. **79**, 685 (1950).
[16] N. Bloembergen and T. J. Rowland, Acta Met. **1**, 731 (1953).
[17] W. H. Jones, Jr., T. P. Graham, and R. G. Barnes, Phys. Rev. **132**, 1898 (1963).
[18] L. H. Mohn and R. G. Barnes (to be published).

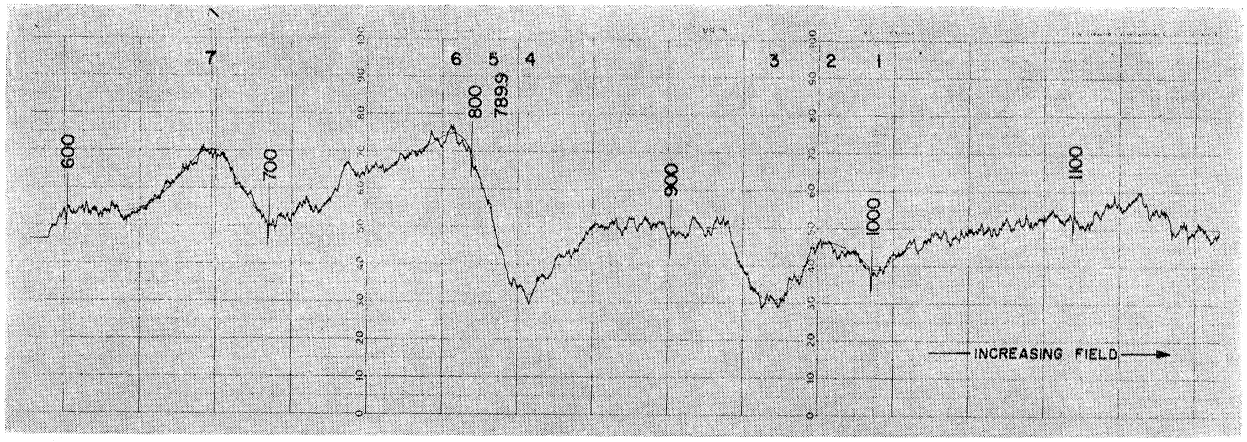

FIG. 1. The NMR absorption derivative recording of La^{139} in polycrystalline lanthanum metal at 15.5020 Mc/sec. The 90° portion of the central $\frac{1}{2}\leftrightarrow-\frac{1}{2}$, transition (peaks No. 4 and No. 6) and one pair of satellite lines (peaks No. 3 and No. 7) are visible. The step, or the 0° portion of the $\frac{1}{2}\leftrightarrow-\frac{1}{2}$ transition, is evidenced by the asymmetric tail on the low field side to peak No. 6. Peaks No. 1 and No. 2 are the La^{139} peaks in LaH_2. The sharp spikes marked 600, 700, 800, etc., are magnetic field calibration points, with 600 corresponding to 25.4825 kOe and 1100–25.7788 kOe.

220°C anneals. Figure 1 shows the recorded pattern after the 200°C anneal. This pattern is that of a first-order quadrupole interaction of the NMR of La^{139} ($I=\frac{7}{2}$) with only the first (innermost) pair of satellite lines visible, peaks No. 3 and No. 7. Note that peaks No. 1 and No. 2 are the absorption derivative peaks of a resonance having the Knight shift (0.236%) of the La^{139} NMR in the fcc structure of LaH_2.[19] The shift of the center of the central peaks No. 4 and No. 6 is 0.643% and is interpreted to be K_H,[17] the shift of that portion of the $\frac{1}{2}\leftrightarrow-\frac{1}{2}$ transition corresponding to $\cos\theta=0$, i.e., arising from those crystallites whose c axis is perpendicular to H_0. The asymmetry of the tail of the central resonance on the low-field side of peak No. 6 is due to the existence of the step in the central transition in a polycrystalline sample,[17] corresponding to $\cos\theta=1$, i.e., to those crystallites whose c axis is parallel or nearly parallel to H_0. The splitting of the central peaks is 21.1±4 Oe. The large uncertainty here results from the use of large magnetic modulation of 18 Oe (peak-to-peak) which was necessary because of the poor signal-to-noise ratio. The separation of the satellite lines is 167.3 Oe or 100.6 kc/sec. This is the lowest pure quadrupole frequency ν_Q and for $I=\frac{7}{2}$, this corresponds to $e^2qQ/h=1.409$ Mc/sec.

The quadrupole perturbation of the Zeeman levels is certainly first order. As was pointed out in a previous paper by the authors,[20] ν_Q is a convenient measure of the quadrupole energy with respect to the Zeeman energy. The relative strength α can be written

$$\alpha=\Delta E_z/\Delta E_Q=\nu_0/\nu_Q=\nu_R(1+K_{\rm iso})/\nu_Q\,, \qquad (1)$$

where ν_0 is the frequency of the center of the Knight shifted resonance pattern, and ν_R is the frequency of the reference solution resonance at fixed field. In this case, $\nu_0=15.5$ Mc/sec and $\nu_Q=0.101$ Mc/sec which means that $\alpha=155$. One can expect second order effects when $\alpha\cong10$ and third-order effects when $\alpha\cong5$.

The quadrupole contribution to the width of the central line is[17] $\Delta\nu_q=b/\nu_0$ where $b=\nu_Q^2[I(I+1)-\frac{3}{4}]/16=0.00956$ (Mc/sec)^2 giving

$$\Delta\nu_q=b/\nu_0=0.617 \text{ kc/sec or } 1.03 \text{ Oe}. \qquad (2)$$

La^{139} has spin $I=\frac{7}{2}$ and there are $2I-1$ or 6 satellite transitions, but only two of these are observed. The reasons for this are plainly that the electric field gradient is inhomogeneous, or alternatively, that there is a distribution of gradient values at the nuclear sites. The second and third pair of satellites are evidently so badly smeared out that they are not detectable.

Several possible factors can contribute to an inhomogeneous field gradient. The first is impurities, atomic and molecular, *in* the lattice. The LaH_2 line is observed in the NMR spectrum. One would expect the LaH_2 to be a surface layer and not an impurity *in* the hcp lattice. The second could be strains which were not removed by annealing, since the annealing stopped at 220°C, as the transformation from hcp to fcc occurs at 260°C.[21] The third is stacking faults produced in the process of filing, and 220°C is certainly below the recrystalization temperature. The stacking faults expected would be layers of the $ABAB$ sequence or the ABC sequence (but other stacking sequences would also be possible) in the so-called double hcp structure of lanthanum which has the $ABAC$ stacking sequence,[21] as shown in Fig. 2. The fourth and final factor (as will be shown in the Appendix) is that the sites in B and C layers in the $ABAC$ stacking have different lattice EFG than the atoms in

[19] D. S. Schreiber and R. M. Cotts, Phys. Rev. **131**, 1118 (1963).
[20] D. R. Torgeson and R. G. Barnes, Phys. Rev. Letters **9**, 255 (1962).
[21] F. H. Spedding, A. H. Daane, and K. W. Herrmann, Acta Cryst. **9**, 559 (1956).

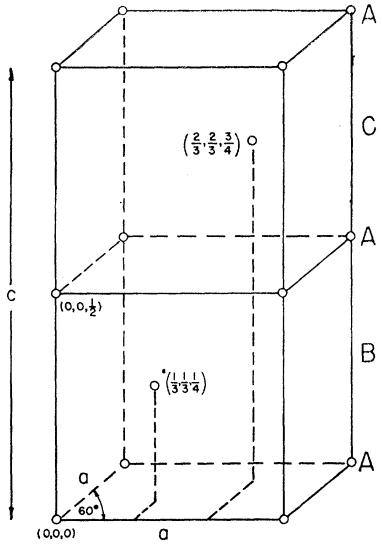

FIG. 2. The unit cell of the *ABAC* stacking sequence of the double hcp structure of lanthanum. The origin is taken at an acute angle in the base following the convention of de Wette (Ref. 24). The unit cell contains four atoms.

the A layers. The point group symmetry at an A site is $\bar{3}m$, and at B and C sites is $\bar{6}m2$.

CALCULATION OF QUADRUPOLE INTERACTION

I. Lattice *EFG*

There are several schemes for calculating the lattice *EFG*,[22–24] but the one most amenable to the *ABAC* hcp structure is the plane-wise summation method of de Wette.[24] We follow the usual convention which is that the electric field gradient eq is defined[24]

$$eq=(\partial^2 V(\bar{r})/\partial z^2)_{r=0}=V_{zz}(0). \tag{3}$$

The double hcp structure of lanthanum (see Fig. 2) has 4 atoms/unit cell at (0,0,0) (the origin of the field gradient calculation and in an A layer), $(\frac{1}{3},\frac{1}{3},\frac{1}{4})$ (a B layer), $(0,0,\frac{1}{2})$ (an A layer), and $(\frac{2}{3},\frac{2}{3},\frac{3}{4})$ (a C layer). These positions are de Wette's notation convention for the hcp cell, in which the origin of the coordinates is taken at an acute interior angle of the cell base rather than at an obtuse angle. To perform the plane-wise summation three different numerical sums are made (see Appendix): $S_{0,0,0}$; $S_{0,0,1/2}$; and $S_{1/3,1/3,1/4}=S_{2/3,2/3,3/4}$. From Spedding *et al.*,[21] $a=3.770$ Å and $c/a=3.2552$. The final result is $q_{2\text{-hcp}}=0.5400\times10^{22}$ cm^{-3} (at an A layer site).

To estimate the effect that large regions of the *ABAB* hcp structure would have on the lattice gradient, we may interpolate in the results of de Wette (Table III of Ref. 24) using $(c/a)/2=1.6126$ from Ref. 21. The result is that $q_{\text{hcp}}=0.5425\times10^{22}$ cm^{-3}, which is within $\frac{1}{2}\%$ of the value at an A layer site in the double hcp structure.

[22] T. P. Das and M. Pomerantz, Phys. Rev. **123**, 2070 (1961).
[23] L. L. Campbell, J. M. Keller, and E. Koenigsberg, Phys. Rev. **84**, 1256 (1951).
[24] F. W. de Wette, Phys. Rev. **123**, 103 (1961).

II. Antishielding Factor

At this point we must distinguish between the lattice *EFG* at the nuclear site eq and the lattice *EFG* that the ion containing the nucleus experiences eq_0. Now eq_0 is produced by all lattice charges not associated with the host ion and can be calculated, given the positions of the lattice charges external to the host ion.[25] It has been demonstrated that $eq=(1-\gamma_\infty)eq_0$, where γ_∞ is the Sternheimer antishielding factor.[26]

Several values of the antishielding factor for La^{3+} have been cited in the literature, and most, if not all, are interpolations of antishielding factors for other ions neighboring La^{3+}. Table I gives a summary of antishielding factors applied to La^{3+}.

TABLE I. Antishielding factor, $\gamma_\infty(La^{139})$.

$\gamma_\infty(La^{139})$	Calculated for:
-143[a]	Cs^+
-110[b]	Cs^+
-105[c]	Pr^{3+}
-78[d]	Pr^{3+}
-74[d]	Tm^{3+}
-73.5[e]	Ce^{3+}

[a] R. M. Sternheimer and H. M. Foley, Phys. Rev. **102**, 731 (1956); D. T. Edmonds, Phys. Rev. Letters **10**, 129 (1963).
[b] E. G. Wikner and T. P. Das, Phys. Rev. **109**, 360 (1958) and Ref. 22.
[c] E. G. Wikner and G. Burns, Phys. Letters **2**, 225 (1962).
[d] Reference 28.
[e] Reference 27.

Freeman and Watson have calculated γ_∞ for Ce^{3+} using unrestricted Hartree-Fock (UHF) functions and get -73.5.[27] Recently, Sternheimer has calculated $\gamma_\infty(Pr^{3+})=-78$ and $\gamma_\infty(Tm^{3+})=-74$.[28] We have chosen Freeman and Watson's value which yields $q=74.5\times0.5135\times10^{22}=38.3\times10^{22}$ cm^{-3}. The value of q_0 used is the average of the A layer value 0.5400×10^{22} and the B or C layer value 0.4870×10^{22}, since there are an equal number of atoms in A layers and B and C layers. It is hoped that in this method the theoretical lattice gradient will more nearly represent the actual lattice gradient.

III. Quadrupole Moment of La^{139}

The values of the nuclear electric quadrupole moment of La^{139} reported in the literature have been many and diverse. Table II gives a summary of the various values.

The most reliable of these values of $Q(La^{139})$ is probably that of Ting's atomic-beam work.[29] Murakawa has proposed[30] a correction of Ting's measured value $Q(La^{139})=(0.23\pm0.01)$ b by the use of an improved (negative) atomic shielding factor (making it an atomic

[25] R. R. Hewett and T. T. Taylor, Phys. Rev. **125**, 524 (1962).
[26] R. M. Sternheimer, Phys. Rev. **84**, 244 (1951); **95**, 736 (1954).
[27] A. J. Freeman and R. E. Watson, Phys. Rev. **132**, 706 (1963).
[28] R. M. Sternheimer, Phys. Rev. **132**, 1637 (1963).
[29] Y. Ting, Phys. Rev. **108**, 295 (1957).
[30] K. Murakawa, Phys. Rev. **110**, 393 (1958).

TABLE II. Quadrupole moment of La^{139}.

$Q(La^{139})$[a] (barn)	Method of determination
0.9 ±0.1[b]	Optical hfs
0.6 ±0.2[c]	Optical hfs
0.3 ±0.1[d]	Optical hfs
0.35 ±0.1[e]	Optical hfs
0.268±0.010[f]	Atomic beam hfs
0.21 ±0.01[g]	Atomic beam hfs[h]
0.21[i]	Optical hfs[i]
	Theoretical determination
0.24[j]	Single particle
0.44[k]	Configuration mixing
0.27[f]	Single particle

[a] Experimental values with and without Sternheimer-type atomic correction factors.
[b] K. Murahawa and T. Kamei, Phys. Rev. **92**, 325 (1953).
[c] K. Murahawa, Phys. Rev. **98**, 1285 (1955).
[d] G. Lührs, Z. Physik **141**, 486 (1955).
[e] K. Murahawa and T. Kamei, Phys. Rev. **105**, 671 (1957).
[f] Reference 29.
[g] See note at end of K. Murakawa, Phys. Rev. **110**, 393 (1958).
[h] This value is based on Ting's measured value and a new atomic shielding correction.
[i] Reference 31.
[j] A. Bohr and B. R. Mottelson, Kgl. Danske Videnskab. Selskab, Mat. Fys. Medd. **27**, No. 16 (1953).
[k] H. Horie and A. Arima, Phys. Rev. **99**, 778 (1955).

antishielding factor) and obtains $Q(La^{139})=0.21$ b. This latter value of Q is further substantiated by later work of Murakawa[31] on the optical hfs of La I, in which he obtains 0.21 b. Freeman and Watson have proposed[27] a negative (ionic) shielding factor, $R=-0.42$ for Ce^{3+}. Recent experimental measurements of the temperature dependence of the quadrupole coupling of Tm^{169} in Tm ethyl sulfate are, however, not compatible with this value of $R=-0.42$.[32] Rather, they indicate that $R(Tm^{3+})=+0.15$ as has been previously believed.[26]

The lattice quadrupole interaction frequency can now be calculated, taking $Q=0.21$ b and $q_0=q_{2\text{-hcp}}$:

$$e^2q_{2\text{-hcp}}(1-\gamma_\infty)Q/h=2.80 \text{ Mc/sec}. \quad (4)$$

This is *larger* than the experimentally observed 1.41 Mc/sec.

SIGN OF CONDUCTION ELECTRON *EFG*

The experimentally observed quadrupole interaction frequency corresponds to a *net* gradient at the nucleus of $q_{\text{exp}}=\pm 19.3\times 10^{22}$ cm^{-3}. One should be reminded that the *nmr* experiment is incapable of determining the sign of the observed gradient, V_{zz} (i.e., of eq_{exp}, or more precisely, of $eq_{\text{exp}}eQ$, but the sign of eQ is known), and so we must allow two cases, i.e., V_{zz} may be positive or negative.

An important question now arises as to the relative sign of the electronic and lattice contributions to the net *EFG*. The lattice contribution to the gradient can be calculated with some confidence, and its sign is therefore known. Das and Pomerantz, in discussing nuclear quadrupole interactions in metals,[22] tacitly assumed the two contributions to be of the same sign. Hewitt and Taylor,[25] however remarked on the possibility that these contributions might have opposite sign in the case of metallic indium.

The net gradient eq_{exp} or $V_{zz}=V_{zz\text{ lat}}+V_{zz\text{ c.e.}}=eq-eq_{\text{c.e.}}$, where eq is the *average* lattice gradient at the nucleus and is produced by an array of positive charges, so that the charge is $+e$. However, the conduction electron gradient, $-eq_{\text{c.e.}}$, is produced by an array of negative charges (electrons) so that the charge is $-e$. In the two cases to be considered, $q_{\text{exp}}=q-q_{\text{c.e.}}$:

Case I: $q_{\text{expI}}=19.3\times 10^{22}$

$$-q_{\text{c.e.I}}=q_{\text{expI}}-q=(19.3-38.3)\times 10^{22}$$
$$=-19.0\times 10^{22} \text{ cm}^{-3}.$$

Case II: $q_{\text{expII}}=-19.3\times 10^{22}$

$$-q_{\text{c.e.II}}=q_{\text{expII}}-q=(-19.3-38.3)\times 10^{22}$$
$$=-57.6\times 10^{22} \text{ cm}^{-3}.$$

In either case the conduction electron *EFG*, $V_{zz\text{ c.e.}}$ is negative, whereas $q_{\text{c.e.}}$ is positive.

One might well calculate $q_{\text{c.e.}}$/electron just as one calculates q_F,[16] the conduction-electron electric field gradient per electron at the Fermi surface, but integrate over all electrons, not just those at the Fermi surface. The full $q_{\text{c.e.}}$ is given by

$$q_{\text{c.e.}}=Z\left\langle \int \psi^* \frac{(3z^2-r^2)}{r^5}\psi d\tau \right\rangle_{k\leq k_F}. \quad (5)$$

It should be pointed out that this method of calculating $q_{\text{c.e.}}$ ignores any antishielding of that portion of the conduction electron outside the host ion, but within the electrically neutral Wigner-Seitz cell. This method of calculating $q_{\text{c.e.}}$ *forces* the sign of $q_{\text{c.e.}}$ and q_F to be the *same*.

KNIGHT SHIFT ANISOTROPY

We derive the Knight shift anisotropy from the shape and position of the central transition at 15.5 Mc/sec. This is done by solving two equations for K_{iso} and a:

$$K_H=K_{\text{iso}}-a+b/\nu_R^2, \quad (6)$$

$$K_s=K_{\text{iso}}+2a, \quad (7)$$

where $K_H=0.643\%$ and is the shift of the mean or average position of lines No. 4 and No. 6, Fig. 1. K_s is the shift of the step (i.e., that portion of the $\frac{1}{2}\leftrightarrow-\frac{1}{2}$ transition in a polycrystalline resonance pattern corresponding to $\cos\theta=1$ or to the c axis parallel to H_0). $K_s=0.777\%$ and is derived from the asymmetry of the low-field tail of the peaks No. 4 and No. 6. The existence of this low-field step is a direct indication of a positive shift anisotropy. From the above equations $a=(0.046\pm 0.020)\%$, and $K_{\text{iso}}=(0.685\pm 0.020)\%$.

[31] K. Murakawa, J. Phys. Soc. Japan **16**, 2533 (1961).
[32] R. G. Barnes, E. Kankeleit, R. L. Mössbauer, and J. M. Poindexter, Phys. Rev. Letters **11**, 253 (1963).

A more satisfying and certainly more precise method of determining K_{ax} (or a) requires the observation of the central transition resonance shape over an extended frequency range. In the present case, attempts to investigate the La^{139} signal at frequencies lower than 15 Mc/sec result in greatly reduced signal-to-noise ratio and loss of resolution. Studies at 12.0 and 13.5 Mc/sec, however, did indicate a rapid increase in apparent line splitting (i.e., the separation of peaks corresponding to No. 4 and No. 6 in Fig. 1) with decreasing frequency, which can also be explained on the basis of a relatively large anisotropy. The term relative refers to the fact that the resonance pattern is influenced by the combined effects of the anisotropic Knight shift and the quadrupole interaction. The relative strength of these interactions has been expressed by Jones *et al.*,[17] as $r=av_0^2/b=11.6$ at 15.5 Mc/sec for lanthanum. Measurements at significantly higher fields are at present limited (in this laboratory) by the 28-kOe maximum field strength available for NMR work.

The Knight shift anisotropy is defined by[14]

$$K_{ax}=\beta^2 V_0 N(E_F) q_F, \tag{8}$$

where β is the Bohr magneton, V_0 is the atomic volume, and $N(E_F)$ is the density of one-electron states at the Fermi level and q_F is as above. From a very simple assumption of the form of the electronic wave function, Borsa and Barnes[33] have shown $q_F=(1/Z)q_{\text{c.e.}}$, assuming the conduction-electronic wave function to have the same form from the bottom to the top of the conduction band. Actually it might be more reasonable to assume that $q_F \geq (1/Zq)_{\text{c.e.}}$ because the wave function certainly changes over the conduction band.

To get $N(E_F)$, we use the electronic specific heat $\gamma=\frac{1}{3}\pi 2k^2 N(E_F)$ which has been measured by low-temperature heat capacity measurements to be, $\gamma=(10.1\pm 0.2)\times 10^4$ erg mole^{-1} (°K)$^{-2}$.[34] Then, from the x-ray work of Spedding *et al.*,[21] one has V_0, so $V_0 N(E_F)=2.67\times 10^{12}$ erg^{-1}, and we can now calculate $q_F=2.0\times 10^{24}$ cm^{-3}, and Zq_F is $\sim$30 times larger than $q_{\text{c.e.}}$ case I, and about 9 times larger than case II.

CONCLUSIONS

The results of these resonance studies do not prove conclusively that filing a chunk of fcc lanthanum, the stable high-temperature phase, automatically produces hcp filings as indicated by Ziegler *et al.*[35] If hcp filings are produced in this way, annealing of the filings for several days at 180°C is required for the initial observation of hcp resonance patterns, strongly suggesting the existence of strains on the as-filed material. On the other hand, the filing process may produce hcp filings and sufficient heat to convert the fresh filings back into the fcc structure. Not until the above mentioned annealing do the filings yield resonance patterns indicative of the hcp structure. X-ray studies performed after each anneal did not yield definitive results about the structure.

The sign of the conduction electron *EFG*, $V_{zz\ \text{c.e.}}$, was demonstrated to be negative. We believe that this case is the only one thus far reported in which $|V_{zz\ \text{exp}}| < |V_{zz\ \text{latt}}|$, and furthermore we believe that only when this inequality is satisfied can the sign of $V_{zz\ \text{c.e.}}$ be determined by nuclear magnetic resonance or by nuclear quadrupole resonance studies.

The existence of two crystallographically dissimiliar lattice sites in the lanthanum double hcp structure results in two different lattice *EFG*. In principle, the existence of two inequivalent lattice sites means also that the conduction electrons move in somewhat different potentials in the neighborhood of the ions at these sites and that the conduction-electron wave functions are periodic in twice the layer spacing in the C direction. In effect, hcp lanthanum can be regarded as an ordered alloy in which all of the atoms happen to be the same. This means that the total *EFG* at the two sites are very likely different, and that, in addition, both the isotropic and anisotropic Knight shifts for the two sites differ somewhat. The experimental results, as well as the calculated values of q_{latt}, suggest that these differences are relatively small.

The recorded resonance pattern is then regarded as a superposition of two patterns, and the Knight shifts and conduction-electron *EFG* values derived must be considered as averages. The average K_{iso} is different, within experimental uncertainty, from $K_{\text{iso}}=(0.64\pm 0.01)\%$ reported by Blumberg *et al.*,[3] for fcc lanthanum metal.

Finally, we conclude that the experiments demonstrate that $q_{\text{c.e.}}$ and q_F have the same sign in the case of lanthanum, although numerical agreement is not obtained. It is apparent that the conduction electron wave functions must change form from the bottom to the top of the conduction band, since $Zq_F > q_{\text{c.e.}}$.

ACKNOWLEDGMENTS

The authors wish to thank Dr. David Peterson for stimulating discussions and assistance in the x-ray analysis. We are indebted to Dr. F. H. Spedding and B. Beaudry for providing the lanthanum metal, and to Ardis Johnson for preparing the samples for NMR study. Helpful discussions with Dr. F. Borsa are gratefully acknowledged.

APPENDIX

We include the details of the calculation of the lattice *EFG* by the plane-wise summation technique of de Wette.[24] As we pointed out above, the double hcp structure of lanthanum metal has four atoms per unit cell. The volume of the unit cell is $(\sqrt{3}/2)a^2c$, the volume

[33] F. Borsa and R. G. Barnes, Phys. Rev. Letters **12**, 281 (1964).
[34] H. Montgomery and G. Pells, Proc. Phys. Soc. (London) **78**, 622 (1961); A. Berman, M. W. Zemansky, and H. A. Boorse, Phys. Rev. **109**, 70 (1958).
[35] W. T. Ziegler, R. A. Young, and A. L. Floyd, J. Am. Chem. Soc. **75**, 1215 (1953).

per ion is $(\sqrt{3}/8)a^2c$. Sums to be considered are $S_{0,0,0}$; $S_{1/3,1/3,1/4}$; $S_{0,0,1/2}$; and $S_{2/3,2/3,3/4}$ for atoms at (0,0,0), $(\frac{1}{3},\frac{1}{3},\frac{1}{4})$, $(0,0,\frac{1}{2})$ and $(\frac{2}{3},\frac{2}{3},\frac{3}{4})$, corresponding to A, B, A, and C layers, respectively. For a definition of the terms, see Ref. 24.

$$S_{0,0,0}=\frac{1}{a^3}\left[-11.0341754+\frac{8\pi^2}{\sqrt{3}}\sum_{\mu_1,\mu_2}\frac{h_{\mu_1,\mu_2}\exp(-\pi h_{\mu_1,\mu_2}\alpha)}{\sinh(\pi h_{\mu_1,\mu_2}\alpha)}\right], \quad \text{(A1)}$$

which can be simplified to the following for calculations:

$$S_{0,0,0}=\frac{1}{a^3}\left[-11.0341754+\frac{8\pi^2}{\sqrt{3}}\sum_i\frac{N_ih_i\exp(-h_i\pi\alpha)}{\sinh(h_i\pi\alpha)}\right]. \quad \text{(A2)}$$

Also,

$$S_{1/3,1/3,1/4}=\frac{8\pi^2}{\sqrt{3}a^3}\sum_{\mu_1,\mu_2}{}'\exp[-\tfrac{2}{3}\pi i(\mu_1+\mu_2)]\times\frac{h_{\mu_1,\mu_2}\cosh(\frac{1}{2}\pi h_{\mu_1\mu_2}\alpha)}{\sinh(\pi h_{\mu_1,\mu_2}\alpha)}, \quad \text{(A3)}$$

which becomes

$$S_{1/3,1/3,1/4}=\frac{8\pi^2}{\sqrt{3}a^3}\sum_i\frac{n_ih_ic_i\cosh(\frac{1}{2}h_i\pi\alpha)}{\sinh(h_i\pi\alpha)}. \quad \text{(A4)}$$

Similarly,

$$S_{2/3,2/3,3/4}=\frac{8\pi^2}{\sqrt{3}a^3}\sum_{\mu_1,\mu_2}\exp[-\tfrac{4}{3}\pi i(\mu_1+\mu_2)]\times\frac{h_{\mu_1,\mu_2}\cosh h(\frac{1}{2}\pi h_{\mu_1,\mu_2}\alpha)}{\sinh(\pi h_{\mu_1,\mu_2}\alpha)} \quad \text{(A5)}$$

becomes

$$S_{2/3,2/3,3/4}=\frac{8\pi^2}{\sqrt{3}a^3}\sum_i\frac{n_ih_ic_i\cosh(\frac{1}{2}h_i\pi\alpha)}{\sinh(h_i\pi\alpha)}, \quad \text{(A6)}$$

so that

$$S_{1/3,1/3,1/4}=S_{2/3,2/3,3/4}. \quad \text{(A7)}$$

Finally,

$$S_{0,0,1/2}=\frac{8\pi^2}{\sqrt{3}a^3}\sum_{\mu_1,\mu_2}{}'\frac{h_{\mu_1,\mu_2}}{\sinh(\pi h_{\mu_1,\mu_2}\alpha)} \quad \text{(A8)}$$

becomes

$$S_{0,0,1/2}=\frac{8\pi^2}{\sqrt{3}a^3}\sum_i\frac{n_ih_i}{\sinh(h_i\pi\alpha)}. \quad \text{(A9)}$$

The results of the numerical sums are

$$\sum_{i=1}^{3}\frac{n_ih_i}{\sinh h_i\pi\alpha}=1.1499262\times10^{-4},$$

$$\sum_{i=1}^{1}\frac{n_ih_i\exp(-h_i\pi\alpha)}{\sinh h_i\pi\alpha}=9.536\times10^{-10}, \quad \text{(A10)}$$

$$2\sum_{i=1}^{9}\frac{n_ih_ic_i\cosh(\frac{1}{2}h_i\pi\alpha)}{\sinh h_i\pi\alpha}=-1.9166754\times10^{-2}.$$

This results in

$$\frac{1}{Z}q_{2\text{-hcp}}=\frac{64\pi}{3a^3}+\frac{1}{a^3}(-11.9010717)=0.001799958\times10^{24}\ \text{cm}^{-3} \quad \text{(A11)}$$

or

$$q_{2\text{-hcp}}=0.539987\times10^{22}\ \text{cm}^{-3}\quad(0.5400\times10^{22}\ \text{cm}^{-3}).$$

One can see very quickly that the lattice *EFG* is the same analytically at the intermediate A layer atom $(0,0,\frac{1}{2})$ of the above discussion by considering reflection of the coordinates in the intermediate plane.

To calculate the gradient at a C layer atom (according to the layer designation above) the atom positions are (using new coordinate frame) (0,0,0), $(\frac{1}{3},\frac{1}{3},\frac{1}{4})$, $(\frac{2}{3},\frac{2}{3},\frac{1}{2})$, and $(\frac{1}{3},\frac{1}{3},\frac{3}{4})$ corresponding to C, A, B and A layers, respectively. We must consider sums $S'_{0,0,0}$, $S'_{1/3,1/3,1/4}$, $S'_{2/3,2/3,1/2}$, and $S'_{1/3,1/3,3/4}$. By definition $S'_{0,0,0}=S_{0,0,0}$ and $S'_{1/3,1/3,1/4}=S_{1/3,1/3,1/4}$. Now

$$S'_{1/3,1/3,3/4}=\frac{8\pi^2}{\sqrt{3}a^3}\sum_{\mu_1,\mu_2}{}'\exp[-\tfrac{2}{3}\pi i(\mu_1+\mu_2)]\times\frac{h_{\mu_1,\mu_2}\cosh(\frac{1}{2}\pi h_{\mu_1,\mu_2}\alpha)}{\sinh(h_{\mu_1,\mu_2}\pi\alpha)}=S_{1/3,1/3,1/4}. \quad \text{(A12)}$$

If $S'_{2/3,2/3,1/2}$ equals $S_{0,0,1/2}$ then the lattice *EFG* is homogeneous; however, this is not the case.

$$S'_{2/3,2/3,1/2}=\frac{8\pi^2}{\sqrt{3}a^3}\sum_{\mu_1,\mu_2}{}'\exp[-\tfrac{4}{3}i\pi(\mu_1+\mu_2)]\times\frac{h_{\mu_1,\mu_2}}{\sinh(h_{\mu_1,\mu_2}\pi\alpha)}, \quad \text{(A13)}$$

which becomes

$$S'_{2/3,2/3,3/4}=\frac{8\pi^2}{\sqrt{3}a^3}\sum_i\frac{n_ih_ic_i}{\sinh h_i\pi\alpha}, \quad \text{(A14)}$$

but

$$S_{0,0,1/2}=\frac{8\pi^2}{\sqrt{3}a^3}\sum_i\frac{n_ih_i}{\sinh h_i\pi\alpha}. \quad \text{(A15)}$$

The result of the numerical sum in $S'_{2/3,2/3,1/2}$ is

$$\sum_{i=1}^{3} \frac{n_i h_i c_i}{\sinh h_i \pi \alpha} = -0.574459 \times 10^{-4}. \quad \text{(A16)}$$

To complete the numerical evaluation, we use the values of the other two sums computed in the calculation of EFG at the A layer site. The numerical result for a B or C layer site, $q_{2\text{-hcp}} = 0.4870 \times 10^{22}$ cm^{-3}, is nearly 10% lower than the A layer site value.

PHYSICAL REVIEW VOLUME 136, NUMBER 3A 2 NOVEMBER 1964

Electron Spin Resonance and Optical Studies on Copper-Doped AgCl

DWIGHT C. BURNHAM AND FRANK MOSER
Research Laboratories, Eastman Kodak Company, Rochester, New York
(Received 3 June 1964)

Upon exposure at room temperature, large, strain-free AgCl crystals containing up to 10^{17} cuprous ions per cm^3 show a stable darkening (print-out) and an electron spin resonance (ESR) absorption which is characteristic of cupric ions. The intensity of the print-out band and of the ESR signal are proportional. Essentially all the cuprous ions are converted to cupric ions by prolonged exposure. For well-annealed crystals, the cupric ESR signal is stable below 180°C in exposed samples and stable below 280°C in halogenated samples, showing that the cuprous ion is a deep hole-trap at room temperature. When the samples are deliberately strained, there are rapid decays in the ESR signal at room temperature. Evidence from ESR suggests that such decays are related to coagulation of cupric ions. Exposure at −180°C converts some cuprous to cupric ions without associated vacancies. Total conversion of cuprous to cupric ions by exposure at room temperature is not obtained in samples containing higher copper concentrations. It is suggested that, at sufficiently high concentrations, cupric ions can compete with intrinsic electron traps, thereby limiting the maximum ESR signal and darkening produced by exposure to smaller values than those expected on the basis of studies of samples with low copper concentration.

I. INTRODUCTION

A NUMBER of studies of the optical,[1] electronic,[2,3] and magnetic effects[4–7] associated with low concentrations of copper ions in large AgCl crystals have been reported. The copper ion in the AgCl lattice can exist in either the cuprous (Cu^{1+}) or the cupric (Cu^{2+}) valence state. These valence states are readily established by heating to about 400°C in nitrogen or chlorine atmospheres, respectively.[8] It is found that the cupric ion produces a broad optical absorption in the visible region (Fig. 1), which is stable in well-annealed crystals but decays in days in strained samples. This decay seems to be produced by some sort of aggregation of the cupric ions. The original cupric absorption band can be restored by heating the sample to about 200°C; this treatment apparently redisperses the cupric ion.[1,4] The cuprous ion adds a weak absorption "tail" to the fundamental absorption edge of AgCl (Fig. 1). Recent studies[3] have clarified the positions of energy levels and the transitions involved in optical absorption and emission associated with the copper ions.

When exposed, pure AgCl crystals do not darken visibly in their volume. AgCl crystals containing cuprous ions darken or "print-out" efficiently at room temperature upon exposure to volume-absorbed light.[1] The absorption produced by exposure is a broad band with the peak near 570 mμ and is stable at room temperature. The strength of the exposure-induced band is initially proportional to the number of absorbed quanta. For concentrations of cuprous ion not exceeding 10^{17}/cm^3, the maximum attainable absorption of the exposure-induced band is proportional to the copper concentration and occurs when the number of volume-absorbed quanta is approximately equal to the number of cuprous ions in the sample.[8] Further exposure, even after a period of dark storage, does not produce significant additional darkening. This behavior is illustrated in Figs. 1 and 2. It was postulated that the cuprous ions act as deep hole-traps at room temperature, forming cupric ions, and that silver ions combine with trapped electrons to form metallic silver. The absorption produced by exposure is then due to the superposition of two absorption bands: one due to silver and one due to cupric ions.

[1] F. Moser, N. R. Nail, and F. Urbach, Phys. Chem. Solids **9**, 217 (1959).
[2] A. M. Gordon, Phys. Rev. **122**, 748 (1961).
[3] R. S. Van Heyningen and F. Moser, Bull. Am. Phys. Soc. **8**, 230 (1963).
[4] R. F. Tucker, Phys. Rev. **112**, 725 (1958).
[5] I. S. Ciccarello, M. B. Palma-Vittorelli, and M. A. Palma, Phil. Mag. **5**, 723 (1960).
[6] L. Bellomonte, M. B. Palma-Vittorelli, and M. A. Palma, Phys. Rev. Letters **9**, 84 (1962); *Proceedings of the First International Conference on Paramagnetic Resonance, Jerusalem, 1962*, edited by W. Low (Academic Press Inc., New York, 1963), Vol. 2, p. 790.
[7] D. C. Burnham and F. Moser, Bull. Am. Phys. Soc. **8**, 231 (1963).
[8] F. Moser, N. R. Nail, and F. Urbach, Phys. Chem. Solids **3**, 153 (1957).

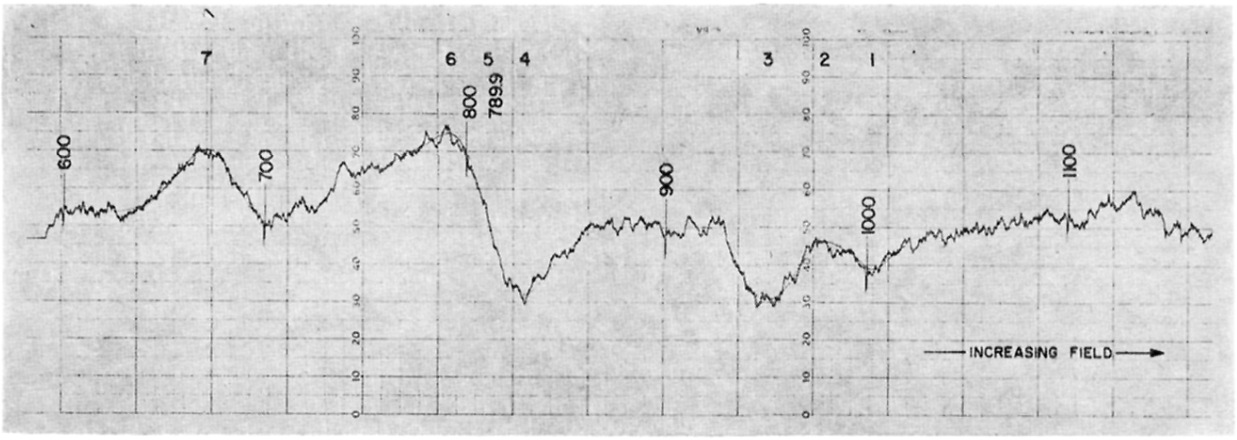

FIG. 1. The NMR absorption derivative recording of La^{139} in polycrystalline lanthanum metal at 15.5020 Mc/sec. The 90° portion of the central $\frac{1}{2} \leftrightarrow -\frac{1}{2}$, transition (peaks No. 4 and No. 6) and one pair of satellite lines (peaks No. 3 and No. 7) are visible. The step, or the 0° portion of the $\frac{1}{2} \leftrightarrow -\frac{1}{2}$ transition, is evidenced by the asymmetric tail on the low field side to peak No. 6. Peaks No. 1 and No. 2 are the La^{139} peaks in LaH_2. The sharp spikes marked 600, 700, 800, etc., are magnetic field calibration points, with 600 corresponding to 25.4825 kOe and 1100–25.7788 kOe.